Theory of the free-electron laser in combined helical pump and axial guide fields

Ira B. Bernstein and Lazar Friedland
Department of Engineering and Applied Science, Yale University, New Haven, Connecticut 06520
(Received 7 July 1980)

The linearized theory of a free-electron-laser amplifier consisting of a relativistic electron beam transported along the axis of a helical wiggler in the presence of an axial guide field is solved exactly. With suitable re-identification of parameters, the theory also applies to the case where the wiggler is replaced by a circularly polarized subluminous radio-frequency pump. The dispersion relation is derived and numerical examples of solutions are presented. These indicate (a) that the use of an axial field permits operation of a laser of given high frequency and undulatory transverse velocity of the unperturbed electron beam at lower values of the pump field, (b) that the gain can be enhanced by approaching the condition of resonance between the effective frequency of the pump and the cyclotron frequency, and (c) that the breadth in frequency of the region corresponding to spatially exponentially growing operation can be much extended.

I. INTRODUCTION

The theory of a free-electron laser (FEL), consisting of a relativistic electron beam transported along the axis of a helical pump magnetic field, has been given by Bernstein and Hirshfield.[1] Their analysis was valid for arbitrary pump strength but weak rf fields, since it involved linearization in the amplitudes of the high-frequency quantities. Here we present the extension of that work to the case where, in addition, there is an axial magnetic field, conventionally present for beam collimation. It is also shown that with a suitable reinterpretation of parameters, the same theory applies when the magnetostatic pump is replaced by a circularly polarized subluminous rf pump. The axial field is shown to yield the additional benefits of permitting the use of weaker pumps, providing enhanced gain and yielding broader domains of spacial instability. This is discussed in detail in Sec. VI.

The work proceeds as follows. The general mathematical description is developed in Sec. II where the continuity and momentum equations describing the relativistic beam, and those governing the electromagnetic fields are presented. Section III describes the properties of a helical pump magnetostatic field, and Sec. IV those of a circularly polarized subluminous rf pump. The linearized equations governing the high-frequency fields are derived in Sec. V. Section VI is devoted to a brief discussion of the relation of this work to its predecessors, to a description of the numerical examples worked out, and conclusions concerning the effects of the axial field.

II. GENERAL MATHEMATICAL DESCRIPTION

Consider a cold relativistic electron beam described by the continuity equation

$$\frac{\partial N}{\partial t} + \nabla \cdot (N\vec{v}) = 0 \qquad (1)$$

and the momentum equation

$$\left(\frac{\partial}{\partial t} + \vec{v}\cdot\nabla\right)(m\gamma\vec{v}) = -e\left(\vec{E} + \vec{v}\times\frac{\vec{B}}{c}\right), \qquad (2)$$

where m is the rest mass of the electron, and

$$\gamma = (1 - v^2/c^2)^{-1/2} \qquad (3)$$

If one forms the scalar product of (2) with $\gamma\vec{v}$ and uses (3) to express v in terms of γ, there results the energy equation

$$\left(\frac{\partial}{\partial t} + \vec{v}\cdot\nabla\right)mc^2\gamma = -e\vec{E}\cdot\vec{v}. \qquad (4)$$

Let $\hat{B}$ be a constant. It is convenient to introduce the electromagnetic potential $\vec{A}$ and Φ via

$$\vec{B} = \hat{B}\vec{e}_z + \nabla\times\vec{A}, \qquad (5)$$

$$\vec{E} = -\nabla\Phi - \frac{\partial}{\partial t}\left(\frac{\vec{A}}{c}\right). \qquad (6)$$

Then with $\Omega = e\hat{B}/mc$ one can write (2) in the form

$$\begin{aligned}\left(\frac{\partial}{\partial t} + \vec{v}\cdot\vec{\nabla}\right)(m\gamma\vec{v}) &= -\left(\frac{e}{c}\right)\left(-c\nabla\Phi - \frac{\partial\vec{A}}{\partial t} + \vec{v}\times(\nabla\times\vec{A}) + \hat{B}\vec{v}\times\vec{e}_z\right)\\ &= m\Omega\vec{e}_z\times\vec{v} + \left(\frac{e}{c}\right)\left(c\nabla\Phi + \frac{\partial\vec{A}}{\partial t} + \vec{v}\cdot\nabla\vec{A} - (\nabla\vec{A})\cdot\vec{v}\right)\end{aligned} \qquad (7)$$

or on rearranging terms

$$\left(\frac{\partial}{\partial t} + \vec{v}\cdot\vec{\nabla}\right)\left(\gamma\vec{v} - \frac{e\vec{A}}{mc}\right) = \Omega\vec{e}_z\times\vec{v} + \left(\frac{e}{mc}\right)[c\nabla\Phi - (\nabla\vec{A})\cdot\vec{v}]. \qquad (8)$$

It follows from the Maxwell equations

$$c\nabla\times\vec{B}=4\pi\vec{J}+\frac{\partial\vec{E}}{\partial t}, \tag{9}$$

$$\nabla\cdot\vec{E}=4\pi\Sigma, \tag{10}$$

on employing (5) and (6), that

$$\nabla^2\vec{A}-c^{-2}\frac{\partial^2\vec{A}}{\partial t^2}+\left(\frac{4\pi}{c}\right)\vec{J}=\nabla\left(c^{-1}\frac{\partial\Phi}{\partial t}+\vec{\nabla}\cdot\vec{A}\right), \tag{11}$$

$$\nabla^2\Phi+4\pi\Sigma=-c^{-1}\nabla\cdot\frac{\partial\vec{A}}{\partial t}. \tag{12}$$

Thus if we adopt the canonical model of FEL theory, viz.

$$\vec{A}=A_x(z,t)\vec{e}_x+A_y(z,t)\vec{e}_y, \tag{13}$$

$$\Phi=\Phi(z,t) \tag{14}$$

(note that the vector potential is written in the Coulomb gauge) and assume that the only charged particles present are electrons, whence $\Sigma=-Ne$ and $\vec{J}=-Ne\vec{v}$, then (11) and (12) yield

$$\frac{\partial^2\vec{A}}{\partial z^2}-c^{-2}\frac{\partial^2\vec{A}}{\partial t^2}=\left(\frac{4\pi Ne}{c}\right)(\vec{v}-\vec{e}_z\vec{e}_z\cdot\vec{v}), \tag{15}$$

$$\frac{\partial^2\Phi}{\partial z^2}=4\pi Ne. \tag{16}$$

III. MAGNETOSTATIC PUMP

Consider the case of a free-electron laser in which the pump magnetostatic field is generated by helical windings and the self-fields of the electron beam are negligible. Then in cylindrical coordinates ρ,θ,z the vacuum magnetic scalar potential χ will be helically invariant, viz.

$$\chi=\chi(\rho,\theta-k_0z), \tag{17}$$

where $2\pi/k_0$ is the pitch, and will satisfy Laplace's equation

$$\nabla^2\chi=\frac{1}{\rho}\frac{\partial}{\partial\rho}\left(\rho\frac{\partial\chi}{\partial\rho}\right)+\left(k_0^2+\frac{1}{\rho^2}\right)\frac{\partial^2\chi}{\partial\theta^2}=0. \tag{18}$$

The general solution of (18), regular at $\rho=0$, on separation of variables is readily shown to be

$$\chi=-\hat{B}z+\sum_{m=1}^{\infty}\chi_m I_m(mk_0\rho)\cos[m(\theta-k_0z)+\lambda_m], \tag{19}$$

where the χ_m and λ_m are constants determined by the details of the helical windings. Recall that the Bessel function

$$I_m(\zeta)=\sum_{s=0}^{\infty}\frac{(\frac{1}{2}\zeta)^{m+2s}}{s!\,(m+s)!}. \tag{20}$$

Thus if a is the radius of the windings and $\rho\ll 2\pi/k_0$, the potential is well approximated by the term with $m=1$ alone, with I_1 approximated by the leading term in the series. The resulting expression for the associated magnetic field is, on choosing the coordinate system so that $\lambda_1=0$ and $\frac{1}{2}k_0\chi_1=-B_0$,

$$\vec{B}=-\nabla\chi\approx\hat{B}\vec{e}_z+B_0(\vec{e}_x\cos k_0z+\vec{e}_y\sin k_0z). \tag{21}$$

The nonconstant part of (21) can be written as the curl of the vector potential

$$\vec{A}=-(B_0/k_0)(\vec{e}_x\cos k_0z+\vec{e}_y\sin k_0z). \tag{22}$$

Expression (22), valid only near the axis, is the form conventionally taken for the magnetostatic pump field. A corresponding solution for the velocity and density can be obtained from (1) and (8) by introducing the basis vectors

$$\vec{e}_1=-\vec{e}_x\sin k_0z+\vec{e}_y\cos k_0z, \tag{23}$$

$$\vec{e}_2=-\vec{e}_x\cos k_0z-\vec{e}_y\sin k_0z, \tag{24}$$

$$\vec{e}_3=\vec{e}_z, \tag{25}$$

when on writing

$$A=A_1\vec{e}_1+A_2\vec{e}_2+A_3\vec{e}_3 \tag{26}$$

it follows that

$$\frac{\partial\vec{A}}{\partial z}=\left(\frac{\partial A_1}{\partial z}-k_0A_2\right)\vec{e}_1+\left(\frac{\partial A_2}{\partial z}+k_0A_1\right)\vec{e}_2+\frac{\partial A_3}{\partial z}\vec{e}_3. \tag{27}$$

Thus (1) and (8) imply

$$\left(\frac{\partial}{\partial t}+\frac{v_3\partial}{\partial z}\right)N=-\frac{N\partial v_3}{\partial z}, \tag{28}$$

$$\left(\frac{\partial}{\partial t}+\frac{v_3\partial}{\partial z}\right)\left(\gamma v-\frac{eA_1}{mc}\right)-k_0v_3\left(\gamma v_2-\frac{eA_2}{mc}\right)=-\Omega v_2, \tag{29}$$

$$\left(\frac{\partial}{\partial t}+\frac{v_3\partial}{\partial z}\right)\left(\gamma v_2-\frac{eA_2}{mc}\right)+k_0v_3\left(\gamma v_1-\frac{eA_1}{mc}\right)=\Omega v_1, \tag{30}$$

$$\left(\frac{\partial}{\partial t}+\frac{v_3\partial}{\partial z}\right)(\gamma v_3)=\left(\frac{e}{mc}\right)\left(\frac{c\partial\Phi}{\partial z}-v_1\frac{\partial A_1}{\partial z}-v_2\frac{\partial A_2}{\partial z}-k_0v_2A_1+k_0v_1A_2\right). \tag{31}$$

Now on combining (22) and (25) one can write

$$\vec{A}_0=(mc^2/e)\xi_0\vec{e}_2, \tag{32}$$

where ξ_0 is a dimensionless constant. It is then readily seen that if also $\Phi_0=0$, corresponding to $E_0=-\nabla\Phi_0=0$, then a solution is given by

$$\vec{v}_0=u\vec{e}_3+w\vec{e}_2, \tag{33}$$

$$N_0=\text{const}, \tag{34}$$

where $u=\text{const}$ and $w=\text{const}$, satisfy (27)–(30) provided that consequent to (29)

$$w=k_0cu\xi_0(k_0u\gamma_0-\Omega)^{-1}: \tag{35}$$

where

$$\gamma_0 = [1-(u^2+w^2)/c^2]^{-1/2} \quad (36)$$

This solution and its experimental accessibility has been analyzed in detail by Friedland.[2]

IV. RADIO-FREQUENCY PUMP

The solution given by (32), (33), and (34) with $\vec{E}_0 = 0$ can also be adapted to describe the case of a free-electron laser with an electromagnetic pump which in the laboratory frame has a phase velocity less than the speed of light. One then views the solution as given in the frame where the pump wave is at rest. Equation (15) then requires, on using (32) and (33), that

$$-k_0^2 c^2 \xi_0 = \omega_p^2 w/c\,, \quad (37)$$

which on using (35) can be written

$$-k_0 c = \omega_p^2 u (k_0 u \gamma_0 - \Omega)^{-1}\,, \quad (38)$$

where the plasma frequency, defined using the rest mass, is

$$\omega_p = (4\pi N_0 e^2/m)^{1/2}\,. \quad (39)$$

Let v_0 be the speed of the laboratory frame as seen from the wave frame. Distinguish quantities in the laboratory frame by a prime. Then on Lorentz transformation $z' = \hat{\gamma}(z - v_0 t)$, $t' = \hat{\gamma}(t - v_0 z/c^2)$, and

$$\omega' = -k_0 v_0 \hat{\gamma}\,, \quad (40)$$

$$k_0' = k_0 \hat{\gamma}\,, \quad (41)$$

where

$$\hat{\gamma} = (1 - v_0^2/c^2)^{-1/2}\,. \quad (42)$$

Clearly

$$v_0 = -\omega'/k_0'\,, \quad (43)$$

is the negative of the phase velocity of the wave. Moreover,

$$\vec{B}_0' = \hat{B}\vec{e}_3 + B_0'[\vec{e}_x \cos(k_0' z' - \omega' t') + \vec{e}_y \sin(k_0' z' - \omega' t')]\,, \quad (44)$$

where

$$B_0' = \hat{\gamma} B_0 \quad (45)$$

and

$$\vec{E}_0' = -(\omega'/k_0' c)\vec{e}_3 \times \vec{B}_0'\,. \quad (46)$$

Evidently the wave is transverse and circularly polarized. The associated potentials are

$$\Phi_0' = 0\,, \quad (47)$$

$$\vec{A}_0' = A_0'[\vec{e}_x \cos(k_0' z' - \omega' t') + \vec{e}_y \sin(k_0' z' - \omega' t')]\,, \quad (48)$$

where

$$A_0' = -\frac{B_0'}{k_0'} = -\frac{B_0}{k_0} = -\frac{mc^2}{e}\xi_0\,. \quad (49)$$

Clearly A_0' is a Lorentz invariant. Also

$$\gamma' = \gamma_0 \hat{\gamma}(1 - v_0 u/c^2)\,, \quad (50)$$

$$N' = N\hat{\gamma}(1 - v_0 u/c^2)\,, \quad (51)$$

$$u' = \frac{u - v_0}{1 - v_0 u/c^2}\,, \quad (52)$$

$$w' = \frac{w/\hat{\gamma}}{1 - v_0 u/c^2}\,. \quad (53)$$

The inverse transformations to (50)–(53) can be gotten by interchanging primed and unprimed variables and changing the sign of v_0.

The counterpart of (35) is now

$$w' = c\xi_0(k_0' u' - c_0')[\gamma_0'(k_0' u - \omega') - \Omega]^{-1}\,. \quad (54)$$

Equation (38) is carried into

$$(\omega'^2 - k_0'^2 c^2) = \omega_P'^2 (k_0' u' - \omega')[\gamma_0'(k_0' u' - \omega') - \Omega]^{-1}\,. \quad (55)$$

Equation (55) can be viewed as the dispersion relation for the pump electromagnetic field, but it is to be noted that the steady-state theory is not restricted to weak pump fields and a linearized theory.

V. STABILITY ANALYSIS

Let us work in the laboratory frame for the case of the magnetostatic pump and in the wave frame for the case of the radio-frequency pump. The stability analysis is then common. Let

$$\vec{A} = \vec{A}_0 - \mathrm{Re}\{(mc^2/e)[\xi_1(z)\vec{e}_1(z) + \xi_2(z)\vec{e}_2(z)]e^{-i\omega t}\}\,, \quad (56)$$

$$\vec{v} = \vec{v}_0 + \mathrm{Re}[\vec{V}(z)e^{-i\omega t}]\,, \quad (57)$$

$$\Phi = 0 + \mathrm{Re}[(mc^2/e)(\omega/kc)\xi_3 e^{-i\omega t}]\,, \quad (58)$$

$$\gamma = \gamma_0 + \mathrm{Re}(\Gamma e^{-i\omega t})\,, \quad (59)$$

$$N = N_0 + \mathrm{Re}(N_1 e^{-i\omega t})\,. \quad (60)$$

Then (29) and (30) yield on linearization

$$\left(-i\omega + u\frac{d}{dz}\right)(\gamma_0 V_1 + c\xi_1) - k_0 u(\Gamma w + \gamma_0 V_2 + c\xi_2) - k_0 V_3(\gamma_0 w - c\xi_0) = -\Omega V_2 \quad (61)$$

$$\left(-i\omega + \frac{ud}{dz}\right)(\Gamma w + \gamma_0 V_2 + c\xi_2) + k_0 u(\gamma_0 V_1 + c\xi_1) = \Omega V_1\,.$$

Rather than use (31) it is convenient to employ the linearized version of (4) which yields

$$\left(-i\omega + \frac{ud}{dz}\right)\Gamma = \left(\frac{\omega u}{kc}\right)\frac{d\xi_3}{dz} + \frac{i\omega w\xi_2}{c}\,. \quad (62)$$

Linearization of (1) gives

$$\left(-i\omega+\frac{ud}{dz}\right)N_1+\left(\frac{d}{dz}\right)(N_0V_3)=0\ , \tag{63}$$

while linearization of (3) implies

$$\Gamma/\gamma_0^3=(uV_3+wV_2)/c^2\ . \tag{64}$$

Equations (15) and (16) on using (27) yield

$$\frac{d^2\xi_1}{dz^2}-k_0^2\xi_1-2k_0\frac{d\xi_2}{dz}+\frac{\omega^2\xi_1}{c^2}=-\frac{\omega_p^2V_1}{c^3}\ , \tag{65}$$

$$\frac{d^2\xi_2}{dz^2}-k_0^2\xi_2+2k_0\frac{d\xi_1}{dz}+\frac{\omega^2\xi_2}{c^2}=-\left(\frac{\omega_p^2}{c^3}\right)\left(V_2+\frac{N_1w}{N_0}\right)\ , \tag{66}$$

$$\frac{\omega}{kc}\frac{d^2\xi_3}{dz^2}=\frac{\omega_p^2}{c^2}\frac{N_1}{N_0}\ . \tag{67}$$

Note that Eqs. (60)–(67) are a system of eight linear ordinary differential equations with constant coefficients for the eight quantities V_1, V_2, V_3, Γ, N_1, ξ_1, ξ_2, and ξ_3. Thus we may seek solutions where all these scalars vary with z as e^{ikz}. If we write

$$\vec{E}=\text{Re}[\vec{a}(z)e^{i\omega t}]\ , \tag{68}$$

then it follows from (6) that

$$\vec{a}=-i(mc\omega/e)\vec{\xi}\ . \tag{69}$$

Equations (60) through (67) then imply

$$i(ku-\omega)(\gamma_0V_1+c\xi_1)-(k_0u-\Omega/\gamma_0)(\gamma_0V_2+c\xi_2+\Gamma w)$$
$$=(\Omega/\gamma_0)c\xi_2+(\Omega/\gamma_0)\Gamma w+k_0V_3(\gamma_0w-c\xi_0)\ , \tag{70}$$

$$(k_0u-\Omega/\gamma_0)(\gamma_0V_1+c\xi_1)$$
$$+i(ku-\omega)(\gamma_0V_2+c\xi_2+\Gamma w)=-(\Omega/\gamma_0)c\xi_1\ , \tag{71}$$

$$\Gamma=\frac{\omega}{c}\frac{u\xi_3+w\xi_2}{ku-\omega}\ , \tag{72}$$

$$\frac{N_1}{N_0}=-\frac{kV_3}{ku-\omega}\ , \tag{73}$$

$$\Gamma=(\gamma_0^3/c^2)(uV_3+wV_2)\ , \tag{74}$$

$$[1-c^2(k_0^2+k^2)/\omega^2]\xi_1-(2ik_0kc^2/\omega^2)\xi_2$$
$$=-(\omega_p^2/\omega^2)(V_1/c)\ , \tag{75}$$

$$(2ik_0kc^2/\omega^2)\xi_1+[1-c^2(k_0^2+k^2)/\omega^2]\xi_2$$
$$=-(\omega_p^2/\omega^2)[(V_2/c)+(w/c)(N_1/N_0)\ , \tag{76}$$

$$N_1/N_0=-(kc\omega/\omega_p^2)\xi_3\ . \tag{77}$$

It is convenient to express Γ, N_1, V_1, V_2, and V_3 in terms of ξ_1, ξ_2, and ξ_3. The result can be represented in the form

$$\underline{\epsilon}\cdot\vec{\xi}=0\ , \tag{78}$$

where the dielectric tensor

$$\underline{\epsilon}=\underline{\theta}+(\omega_p^2\tau/\gamma_0\omega^2)\underline{\psi} \tag{79}$$

and

$$\tau=(\Omega/\gamma_0)[(ku-\omega)^2-(k_0u-\Omega/\gamma_0)^2]^{-1}\ . \tag{80}$$

The components of θ are

$$\theta_{11}=1-c^2(k_0^2+k^2)/\omega^2-\omega_p^2/\gamma_0\omega^2\ ,$$
$$\theta_{13}=\theta_{31}=0\ ,$$
$$\theta_{12}=-\theta_{21}=-2ic^2k_0k/\omega^2\ ,$$
$$\theta_{22}=1-c^2(k_0^2+k^2)/\omega^2 \tag{81}$$
$$-(\omega_p^2/\gamma_0\omega^2)[1+(w^2/c^2)(k^2c^2-\omega^2)(ku-\omega)^{-2}]\ ,$$
$$\theta_{23}=\theta_{32}=-(\omega_p^2/\gamma_0)(ku-\omega)^{-2}(w/\omega)(k-\omega u/c^2)\ ,$$
$$\theta_{33}=1-(\omega_p^2/\gamma_0)(ku-\omega)^{-2}(1-u^2/c^2)\ .$$

The elements of $\underline{\psi}$ are

$$\psi_{11}=k_0u-\Omega/\gamma_0\ ,$$
$$\psi_{12}=-i(ku-\omega)\left(1+\frac{w^2}{c^2}\frac{\omega}{ku-\omega}\right)\ ,$$
$$\psi_{13}=-i(ku-\omega)\left(\frac{uw}{c^2}\frac{\omega}{ku-\omega}+\frac{\xi_0k_0c\omega}{\omega_p^2}\frac{ku-\omega}{k_0u-\Omega/\gamma_0}\right)\ ,$$
$$\psi_{21}=i\left(\frac{k(u^2+w^2)}{u}-\omega\right)\ , \tag{82}$$
$$\psi_{22}=\left(\frac{k(u^2+w^2)}{u}-\omega\right)\frac{k_0u-\Omega/\gamma_0}{ku-\omega}\left(1+\frac{w^2}{c^2}\frac{\omega}{ku-\omega}\right)\ ,$$
$$\zeta_{23}=\left(\frac{k(u^2+w^2)}{u}-\omega\right)\frac{k_0u-\Omega/\gamma_0}{ku-\omega}$$
$$\times\left(\frac{uw}{c^2}\frac{\omega}{ku-\omega}+\frac{\xi_0k_0c\omega}{\omega_p^2}\frac{ku-\omega}{k_0u-\Omega/\gamma_0}\right)\ ,$$
$$\psi_{31}=i\omega w/u\ ,$$
$$\psi_{32}=\frac{\omega w}{u}\frac{k_0u-\Omega/\gamma_0}{ku-\omega}\left(1+\frac{w^2}{c^2}\frac{\omega}{ku-\omega}\right)\ ,$$
$$\psi_{33}=\frac{\omega w}{u}\frac{k_0u-\Omega/\gamma_0}{ku-\omega}\left(\frac{uw}{c^2}\frac{\omega}{ku-\omega}+\frac{\xi_0k_0c\omega}{\omega_p^2}\frac{ku-\omega}{k_0u-\Omega/\gamma_0}\right)\ .$$

In the limit $\Omega\to 0$, τ vanishes and $\underline{\epsilon}$ reduces to $\underline{\theta}$, which apart from notation is the form found by Bernstein and Hirshfield.[1]

VI. THE DISPERSION RELATION AND NUMERICAL EXAMPLES

In order that (78) have nontrivial solutions it is necessary that the determinant

$$D=\det\underline{\epsilon}=0\ . \tag{83}$$

This yields an eighth-order polynomial equation for k. In practice, for the cases of interest $\omega_p^2\ll\omega^2$ and $u\sim c$, and two of the roots are such that $\omega/k\approx -c$. That is, they propagate in the negative-z direction counter to the beam and are substantially unaffected by the tenuous beam. The remaining six roots correspond to waves which propagate along the beam. When $\Omega \to 0$ the two of these which can be associated with cyclotron waves in the limit of no helical pump disappear, and one recovers the result of Bernstein and Hirshfield.[1] These features will be illustrated later when numerical examples are discussed.

Now Eqs. (61)–(67) comprise a tenth-order system of linear ordinary differential equations which require for a unique solution the stipulation of ten boundary conditions. Since usually there is negligible reflection of waves at the output end of an FEL amplifier of finite length, two conditions are the requirement that the amplitudes of the waves propagating counter to the beam be zero. This requirement can be most easily dealt with via solving the system of ordinary differential equations by means of a Laplace transform in z, as was done in Ref. 1, instead of the normal mode analysis. The dispersion relation, of course, determines the poles of the transform in terms of which the inversion can be readily accomplished. The resulting solution for $\vec{a}(z)$ can be written in terms $\vec{a}(0)$, assuming that all other first-order quantities are zero at $z=0$ and involve linear combinations of the six modes corresponding to the six roots with $\text{Re}k>0$. Since in general these roots are nondegenerate, but differ by amounts of order Δk much less than ω/c, there will be interference amongst their contributions to $\vec{a}(z)$, which becomes evident after a distance of order $2\pi/\Delta k$. This feature has been examined in detail in Ref. 1. We will not pursue it further here, other than to note that the single particle theory in which one examines the second-order energy change in a distance z of an electron moving in the zero- and first-order electromagnetic field, and identifies this with the gain in energy of the high frequency field, is valid only for $z\Delta k<1$.

We now consider the dispersion relation (83) in an FEL with guide magnetic field. Because of the complexity of the dielectric tensor $\underline{\epsilon}$ [see Eq. (79)] it is convenient to study the dispersion relation by comparing two FEL's, identical except that one has an axial field while the second does not and thus is characterized by the dispersion relation $D_0=\det(\underline{\theta})=0$, the properties of which are well understood. We make the comparison between the two lasers by fixing the parameters of the FEL without the guide field and adjusting the value of the pump field parameter ξ_0 in the laser with the guide field so that the axial velocities u (and therefore also w) in both lasers are identical. This assures the same Doppler upshift of the frequencies in the lasers. A similar comparison has been made by Friedland and Hirshfield for the single particle model of FEL.[3]

Let ξ_0^0 be the pump field parameter in the FEL without the guide field. The unperturbed electron velocity components are then given by $w/c=\xi_0^0/\gamma_0$ and $u/c=[1-(1+\xi_0^0)/\gamma_0^2]^{1/2}$. Therefore, following Eq. (35), with the guide field

$$\xi_0=\xi_0^0\left(1-\frac{\Omega}{\gamma_0 k_0 u}\right). \tag{84}$$

This equation demonstrates the intriguing possibility of reduction of the pump field in an FEL as one approaches the cyclotron resonance condition $\Omega/\gamma_0 \to k_0 u$. Accessibility of the resonance, however, is not guaranteed, as was shown in the recent study[2] of the unperturbed electron beam orbits in an FEL with the guide field. It was demonstrated that for given values of γ_0, k_0, ξ_0, and Ω the electrons can possess more than one steady state. For example, Fig. 1 shows u/c versus Ω/c for $k_0=6\text{ cm}^{-1}$, $\gamma_0=3$, and $\xi_0=0.5$. For $\Omega>\Omega_{cr}$ it is seen that only one branch exists (branch C). But when $\Omega<\Omega_{cr}$ two additional branches (A and B) are allowed. It was also shown that the necessary condition for orbital stability of the steady-state solutions against small perturbations is given by the inequality

$$\frac{\Omega}{ck_0\xi_0}\left(\frac{w}{u}\right)^3<1. \tag{85}$$

Branch C is always stable, since $w<0$ on this branch. On branches A and B, $w>0$, but, as was shown, only branch A satisfied (85) and thus may be used in applications. Since the ratio w/u is kept constant in our comparative study, one can substitute the expression for ξ_0 found from (35) into (85) and write the stability condition in the following form:

$$\Omega<\Omega_{cr}=\frac{\gamma_0 k_0 u}{1+(w/u)^2}, \tag{86}$$

valid for branches A and B. In our sample case ($\gamma_0=3$, $k_0=6\text{ cm}^{-1}$, and $\xi_0^0=0.5$) one has $\Omega_{cr}/c=16.18\text{ cm}^{-1}$, and, therefore, according to (84),

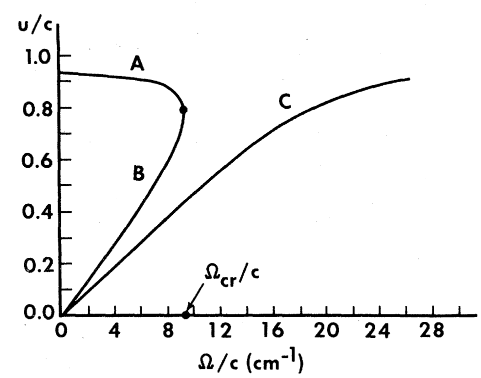

FIG. 1. Steady-state normalized axial velocity u/c as a function of normalized axial magnetic field Ω/c.

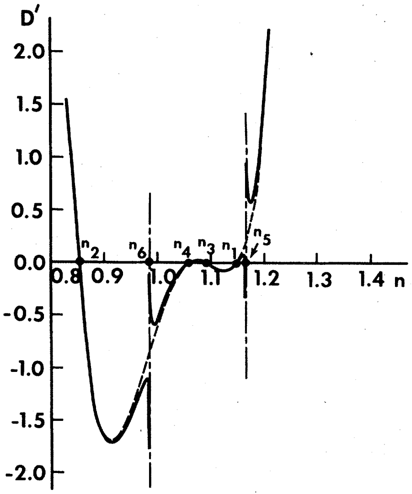

FIG. 2. Dispersion function D' on branch A for the case $\gamma_0=3$, $k_0=6\ \mathrm{cm}^{-1}$, and $\omega/c=40\ \mathrm{cm}^{-1}$. The dashed curve represents the FEL without the guide magnetic field and $\xi_0^0=0.5$. The solid curve is for the FEL with the guide field ($\Omega/c=6.5\ \mathrm{cm}^{-1}$), where smaller values of ξ_0^0 are used so as to provide the same values of u and w as for the dashed curve.

ξ_0 on branch A cannot become less than $\xi_{cr}=1.562\times 10^{-2}$.

We return now to the study of the dispersion relation (83). The form of the dielectric tensor $\underline{\epsilon}$ [Eq. (79)] suggests that for values of ω_p small enough, the function D will differ significantly from D_0 only in the regions where $(ku-\omega)^2-(k_0u-\Omega/\gamma_0)^2\simeq 0$, as a result of the resonance in the denominator in τ [see Eq. (80)]. We demonstrate a typical effect of the axial guide field on the dispersion function D in Fig. 2, where the function $D'=D[ku-\omega)/\omega_p(1-u^2/c^2)]^2/\gamma_0$ (the full line) is shown versus $n=ck/\omega$ for branch A in the sample case when $\omega/c=40\ \mathrm{cm}^{-1}$, $\omega_p^2/c^2=0.5\ \mathrm{cm}^{-2}$, and $\Omega/c=6.5\ \mathrm{cm}^{-1}$. In the same figure the dashed line represents the case with no guide field.

It is well known[1] that the unstable regime in an FEL without the guide field can be described as a coupling between the transverse electromagnetic modes with the dispersion relation $n_{1,2}=1\pm ck_0/\omega$ and the electrostatic beam modes characterized by $n_{3,4}=c/u\pm c\omega_p/\gamma_0\omega u$. One can see from Fig. 2 that these four roots are only slightly perturbed by the presence of the axial field. There exist, however, two additional roots in the neighborhood of the resonance points $n_{5,6}=c/u\pm(ck_0/\omega-\Omega c/\gamma u\omega)$. If the resonances are widely separated as in the case of Fig. 2, the onset of the unstable mode is roughly the same as without the guide field, namely, as the frequency ω increases, the root n_1 moves to 1, passing the region $n_4<n<n_3$ (since $n_{3,4}\to c/u$). The modes couple in this region,

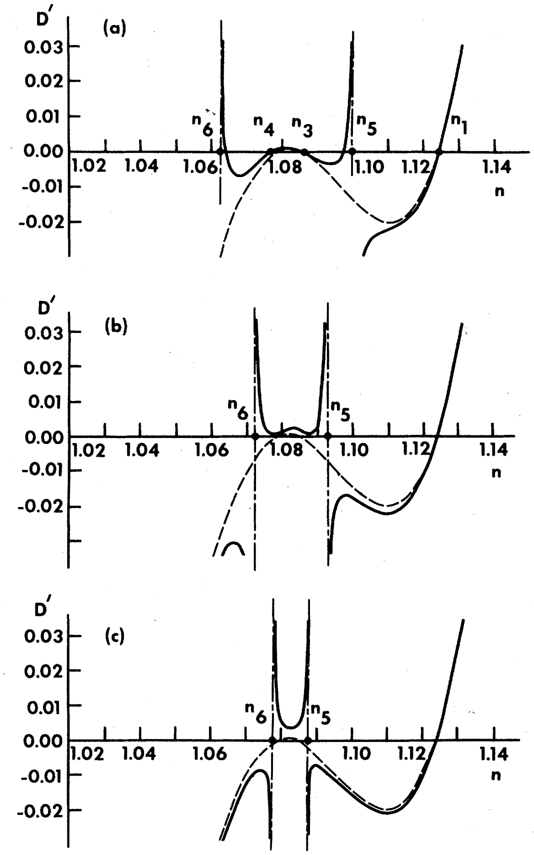

FIG. 3. Graphical representation of the dispersion function on branch A for the case $\gamma_0=3$, $k_0=6\ \mathrm{cm}^{-1}$, $\xi_0^0=0.5$, $\omega/c=50\ \mathrm{cm}^{-1}$, and increasing values of the guide field (the solid curves): (a) $\Omega/c=14\ \mathrm{cm}^{-1}$, (b) $\Omega/c=15\ \mathrm{cm}^{-1}$, (c) $\Omega/c=16\ \mathrm{cm}^{-1}$. The dashed curves correspond to the FEL without the guide field. Two pairs of roots of the dispersion relation become complex as the real roots n_3 and n_4 are squeezed by the resonances at n_5 and n_6.

and the roots of the dispersion relation are complex. When ω continues to increase, n_1 becomes less than n_4, the coupling diminishes, and one again has a stable regime.

New effects may occur when the resonances $n_{5,6}$ approach each other. This situation is shown in Fig. 3, where the full line represents the dispersion function on branch A for increasing values of Ω. One can see in this example that even for $\omega/c=50\ \mathrm{cm}^{-1}$ in our sample case (all the modes are stable in this case if $\Omega=0$) it is possible just by changing Ω to squeeze the roots $n_{3,4}$ by the resonances $n_{5,6}$ so that two pairs of the roots become complex. For higher frequencies, when again the FEL without the guide field is stable ($n_1<n_4$) one can also get an unstable regime as is demonstrated in Fig. 4 for $\omega/c=100\ \mathrm{cm}^{-1}$. Our numerical study

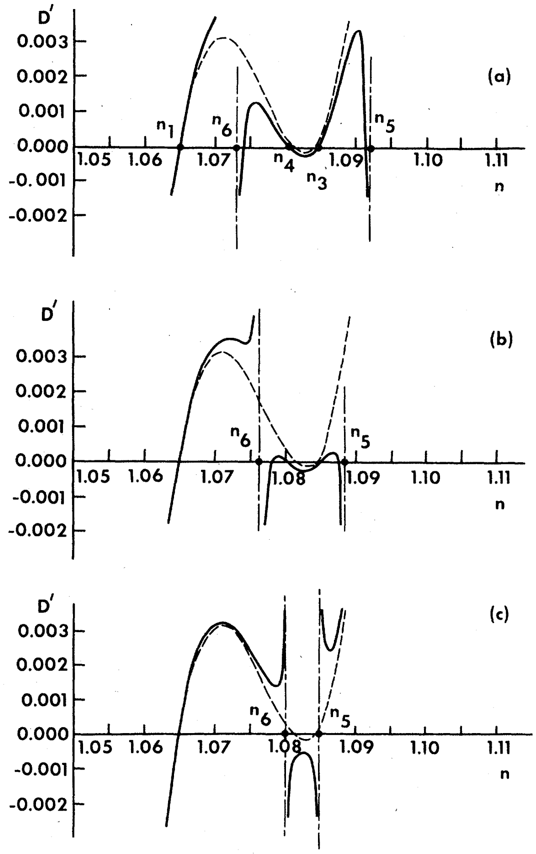

FIG. 4. Graphical representation of the dispersion function on branch A for the case $\gamma_0=3$, $k_0=6$ cm^{-1}, $\xi_0^0=0.5$, $\omega/c=100$ cm^{-1}. The solid curves: (a) $\Omega/c=14$ cm^{-1}; (b) $\Omega/c=15$ cm^{-1}; (c) $\Omega/c=16$ cm^{-1}. The dashed curves correspond to the FEL without the guide field.

shows that similar behavior is also characteristic for branch C with the only difference that there is only one pair of unstable modes in the low and the high frequency ranges, respectively.

We finally summarize our comparison of the FEL's with and without the guide field in Figs. 5 and 6, where the imaginary part of k is shown as a function of ω/c for various values of the axial field in our sample case ($\gamma_0=3$, $k_0=6$ cm^{-1}, $\xi_0^0=0.5$, $\omega_p^2/c^2=0.5$ cm^2). Figure 5 is for $0<\Omega/c<14.5$ cm^{-1} on branch A (the full lines) and $21<\Omega/c<28$ cm^{-1} on branch C (the dashed lines). The resonances $n_{5,6}$ are relatively wide apart from each other and formally the instability in this range of Ω occurs similarly to the case of the laser without the guide field. Nevertheless, the presence of the guide field increases the instability on branch A and tends to decrease it on branch C. In addition, the linewidth of the unstable regime is seen to be significantly increased at lower frequencies on branch A. Together with this, no instability exists at frequencies higher than those

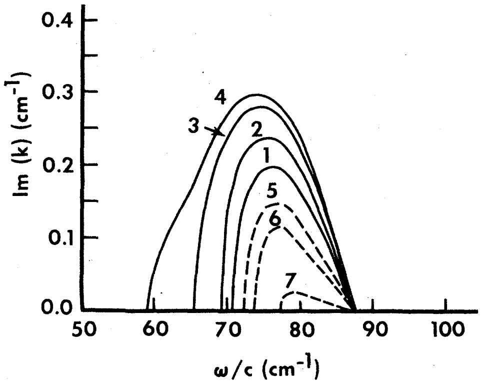

FIG. 5. Spacial growth rates Im(k) versus ω/c on branch A (solid curves) and C (dashed curves) for various values of Ω/c: (1) $\Omega/c=0$, (2) $\Omega/c=12$ cm^{-1}, (3) $\Omega/c=14$ cm^{-1}, (4) $\Omega/c=14.5$ cm^{-1}, (5) $\Omega/c=28$ cm^{-1}, (6) $\Omega/c=23$ cm^{-1}, (7) $\Omega/c=21$ cm^{-1}. For all the cases $\gamma_0=3$, $k_0=6$ cm^{-1}, and $\xi_0^0=0.5$.

characteristic of the FEL without the guide field. As one approaches the resonance condition $\Omega=\gamma_0 u k_0$ (further increasing Ω on branch A or decreasing it on branch C) a completely different type of behavior is observed as is shown in Fig. 6 for $\Omega/c=15.25$ cm^{-1} on branch A (the full line) and $\Omega/c=18$ cm^{-1} on branch C (the dashed line). The unstable region extends over the entire low-frequency range and there are two different unstable modes on branch A, as was mentioned previously. In addition there exist unstable modes in the high-frequency region, which was totally stable before. Note that the values of Imk in this high-frequency regime are only weakly dependent on the frequency itself.

Thus, in conclusion, we have demonstrated in

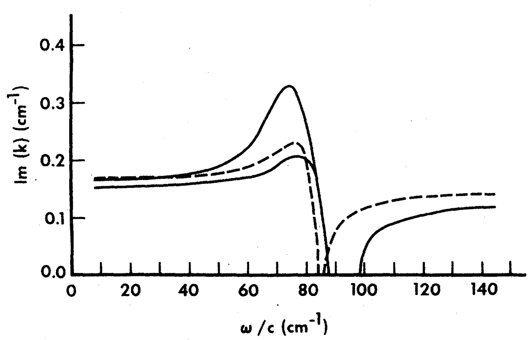

FIG. 6. Spatial growth rates Im(k) in the sample case ($\gamma_0=3$, $k_0=6$ cm^{-1}, $\xi_0^0=0.5$) versus ω/c in the regime, where the cyclotron modes couple to the beam modes (see Figs. 3,4). Branch A (solid curves): $\Omega/c=15.25$ cm^{-1}. Branch C (dashed curves): $\Omega/c=18$ cm^{-1}. The unstable modes are extended over the low- and high-frequency regions. There exist two different growth constants in this regime on branch A.

our numerical examples that the presence of the guide field in an FEL introduces the following desirable features:

(i) One can operate the laser with much lower magnitudes of the pump field without sacrificing the undulatory velocity of the electrons. This allows one to use shorter periods of the wiggler with the same currents.

(ii) The laser can be operated in higher gain regime by approaching the resonance condition $\Omega = k_0 u \gamma_0$.

(iii) The linewidth of the unstable modes can be widely extended to both low- and high-frequency ranges.

ACKNOWLEDGMENT

This work was supported by the Office of Naval Research and by the National Science Foundation.

[1] I. B. Bernstein and J. L. Hirshfield, Phys. Rev. A 20, 1661 (1979).

[2] L. Friedland, Phys. Fluids 23, 2376 (1980).

[3] L. Friedland and J. L. Hirshfield, Phys. Rev. Lett. 44, 1456 (1980).